



AFRL-RX-WP-JA-2014-0230

**INVESTIGATION OF ACOUSTIC FIELDS GENERATED
BY EDDY CURRENTS USING AN ATOMIC FORCE
MICROSCOPE (POSTPRINT)**

**V. Nalladega and S.Sathish
University of Dayton Research Institute**

**M. Blodgett
AFRL/RXCA**

**AUGUST 2012
Interim Report**

Distribution A. Approved for public release; distribution unlimited.

See additional restrictions described on inside pages

STINFO COPY

© 2013 American Institute of Physics

**AIR FORCE RESEARCH LABORATORY
MATERIALS AND MANUFACTURING DIRECTORATE
WRIGHT-PATTERSON AIR FORCE BASE, OH 45433-7750
AIR FORCE MATERIEL COMMAND
UNITED STATES AIR FORCE**

REPORT DOCUMENTATION PAGE

Form Approved
OMB No. 074-0188

Public reporting burden for this collection of information is estimated to average 1 hour per response, including the time for reviewing instructions, searching existing data sources, gathering and maintaining the data needed, and completing and reviewing this collection of information. Send comments regarding this burden estimate or any other aspect of this collection of information, including suggestions for reducing this burden to Defense, Washington Headquarters Services, Directorate for Information Operations and Reports, 1215 Jefferson Davis Highway, Suite 1204, Arlington, VA 22202-4302. Respondents should be aware that notwithstanding any other provision of law, no person shall be subject to any penalty for failing to comply with a collection of information if it does not display a currently valid OMB control number. PLEASE DO NOT RETURN YOUR FORM TO THE ABOVE ADDRESS.

1. REPORT DATE (DD-MM-YYYY) August 2012		2. REPORT TYPE Interim		3. DATES COVERED (From - To) 25 June 2009 - 15 July 2012	
4. TITLE AND SUBTITLE INVESTIGATION OF ACOUSTIC FIELDS GENERATED BY EDDY CURRENTS USING AN ATOMIC FORCE MICROSCOPE (POSTPRINT)				5a. CONTRACT NUMBER FA8650-09-D-5224-0001	
				5b. GRANT NUMBER	
				5c. PROGRAM ELEMENT NUMBER 62102F	
6. AUTHOR(S) (see back)				5d. PROJECT NUMBER 4347	
				5e. TASK NUMBER	
				5f. WORK UNIT NUMBER X0SU	
7. PERFORMING ORGANIZATION NAME(S) AND ADDRESS(ES) (see back)				8. PERFORMING ORGANIZATION REPORT NUMBER	
9. SPONSORING / MONITORING AGENCY NAME(S) AND ADDRESS(ES) Air Force Research Laboratory Materials and Manufacturing Directorate Wright Patterson Air Force Base, OH 45433-7750 Air Force Materiel Command United States Air Force				10. SPONSOR/MONITOR'S ACRONYM(S) AFRL/RXCA	
				11. SPONSOR/MONITOR'S REPORT NUMBER(S) AFRL-RX-WP-JA-2014-0230	
12. DISTRIBUTION / AVAILABILITY STATEMENT Distribution A. Approved for public release; distribution unlimited. This report contains color.					
13. SUPPLEMENTARY NOTES Journal article published in AIP Conf. Proc. 1511, 449-455 (2013). © 2013 American Institute of Physics 978-0-7354-1129-6. The U.S. Government is joint author of the work and has the right to use, modify, reproduce, release, perform, display or disclose the work. The final publication is available at doi: 10.1063/1.4789082. If authorized, also see also AFRL-RX-WP-TR-2014-0218.					
14. ABSTRACT This paper reports the experimental measurement and imaging of the acoustic fields generated by low-frequency eddy currents in metals in the absence of an external static magnetic field using a modified atomic force microscope. Acoustic displacements in a typical metal placed in eddy current field without static magnetic field were theoretically computed and found to be in the range of few hundred picometers. A modified atomic force microscope was used to detect and measure the acoustic displacements in a single crystal copper. The setup was also used to image acoustic fields in a titanium alloy sample. Details of the modified AFM to measure and image acoustic displacements are presented. The role of electrical and elastic properties on the contrast in acoustic images of Ti-6Al-4V sample is discussed.					
15. SUBJECT TERMS acoustic fields, eddy currents, atomic force microscopy					
16. SECURITY CLASSIFICATION OF:			17. LIMITATION OF ABSTRACT	18. NUMBER OF PAGES	19a. NAME OF RESPONSIBLE PERSON (Monitor) John T. Welter
a. REPORT Unclassified	b. ABSTRACT Unclassified	c. THIS PAGE Unclassified			SAR

REPORT DOCUMENTATION PAGE Cont'd

6. AUTHOR(S)

V. Nalladega and S.Sathish - University of Dayton Research Institute

M. Blodgett - Materials and Manufacturing Directorate, Air Force Research Laboratory, Structural Materials Division

7. PERFORMING ORGANIZATION NAME(S) AND ADDRESS(ES)

University of Dayton Research Institute
Structural Integrity Division
300 College Park Drive
Dayton OH 45469

AFRL/RXCA
Air Force Research Laboratory
Materials and Manufacturing Directorate
Wright-Patterson Air Force Base, OH 45433-7750

INVESTIGATION OF ACOUSTIC FIELDS GENERATED BY EDDY CURRENTS USING AN ATOMIC FORCE MICROSCOPE

V. Nalladega¹, S.Sathish¹, and M. Blodgett²

¹Structural Integrity Division, University of Dayton Research Institute, 300 College Park, Dayton OH 45469

²Metals, Ceramics, and NDE Division, Air Force Research Laboratory, Wright Patterson Air Force Base, OH 45433

ABSTRACT. This paper reports the experimental measurement and imaging of the acoustic fields generated by low-frequency eddy currents in metals in the absence of an external static magnetic field using a modified atomic force microscope. Acoustic displacements in a typical metal placed in eddy current field without static magnetic field were theoretically computed and found to be in the range of few hundred picometers. A modified atomic force microscope was used to detect and measure the acoustic displacements in a single crystal copper. The setup was also used to image acoustic fields in a titanium alloy sample. Details of the modified AFM to measure and image acoustic displacements are presented. The role of electrical and elastic properties on the contrast in acoustic images of Ti-6Al-4V sample is discussed.

Keywords: Acoustic Fields, Eddy Currents, Atomic Force Microscopy

PACS: 07.79.Lh, 43.35.-c

INTRODUCTION

It is well known that acoustic fields can be generated in a metallic sample placed in an electromagnetic field [1]. This phenomenon has led to the development of electromagnetic acoustic transducers (EMAT) for nondestructive evaluation of metals [2-5]. The major advantage of an EMAT transducer is that a direct contact between the coil and the sample is not necessary and hence no need for an acoustic couplant. In an electromagnetic acoustic transducer, the acoustic fields are generated by the mechanical body forces due to Lorentz forces [6]. Lorentz forces are generated due to the interaction of the eddy currents with the magnetic field of the coil. Typical EMATs used for NDE applications and physical acoustics studies frequently use an external bias static magnetic field in addition to the coil's magnetic field [1-6] to enhance the acoustic displacements in the metal.

While a static magnetic field is often used in a typical EMAT configuration, theoretical arguments regarding the generation of acoustic fields in the absence of an external static magnetic field have been reported [7-9]. In such cases, the acoustic field is generated only due to the dynamic magnetic field of a coil and its amplitude is usually small. Therefore, in the conventional EMAT configurations where an external static

magnetic field is used, the Lorentz force contribution from dynamic magnetic field of the coil is ignored and the strong static field is considered. However, in a recent study, it has been shown that the contribution of the dynamic magnetic field to the Rayleigh wave amplitude is comparable to the static magnetic field contribution [5] and has been used to enhance the efficiency of the EMAT. In another study, the concept of acoustic wave generation due to eddy currents in the absence of external static magnetic field was discussed [9]. In both cases, large currents have to be used in order to generate acoustic displacements that can be measured either by another coil or a laser interferometer. It is important to note that in the absence of external magnetic field only longitudinal waves can be generated in the metal. Several research groups [7, 8, 10] have shown that acoustic waves at twice the exciting frequency are generated in metal when excited by an electromagnetic coil driven at large currents, in the absence of external static magnetic field. Therefore, it can be seen that in order to detect the acoustic displacements in the absence of external static magnetic field, large excitation currents are necessary. A literature survey shows that there are not many studies that have dealt with the detection of acoustic displacements in metals due to eddy currents in the absence of an external magnetic field *and* especially with low excitation currents. Since the acoustic amplitudes are small at low currents, the conventional techniques have serious limitations to detect such small amplitudes. One of the techniques that can be used to detect very small displacements is atomic force microscopy (AFM).

AFM is a popular technique used to image surfaces of both conductors and insulators with nanometer spatial resolution [11]. In addition to routine topography imaging, AFM can also be used to measure and image physical properties of the material [12-14]. This requires modifications to the AFM so that both topography and the physical property can be imaged simultaneously.

Although theoretical analysis of the acoustic displacements due to eddy currents in the presence of an external static magnetic field has been extensively studied, very few studies are reported for the theoretical calculation of acoustic displacements in the absence of a static magnetic field. Moreover, experimental detection of acoustic displacements at low excitation currents and zero static magnetic field are not reported in the literature. This paper discusses the application of a modified AFM to detect and image acoustic displacements in a metal subjected to low frequency electromagnetic field in the absence of an external magnetic field. Acoustic displacements were measured using a flexible cantilever of an AFM in a copper sample as a function of input current to the coil. The theoretical results are compared with the experimental measurements on the copper. The modifications to the AFM to image acoustic fields due to eddy currents are discussed. As an application for the imaging, the technique was used to image the microstructure of a titanium alloy, Ti-6Al-4V. The contrast seen in the images are discussed based on the local variation of the electrical conductivity and elastic properties of Ti-6Al-4V.

THEORY

When a metallic sample is placed in the field of a time-varying current, eddy currents are induced in the metallic sample within the skin depth. The eddy currents produce a dynamic magnetic field within the sample. This dynamic magnetic field interacts with the eddy currents producing body forces in the sample known as Lorentz force. In the case of nonmagnetic metals, the Lorentz force, F is given by

$$F = J \times B \quad (1)$$

where J is the eddy current density and B is the magnetic field. The Lorentz force for an EMAT configuration can be expressed as

$$F = F_s + F_d \quad (2)$$

where F_s and F_d are static and dynamic Lorentz forces caused by static and dynamic magnetic fields respectively. In the absence of an external static magnetic field the Lorentz force is caused only by the interaction of eddy currents with the dynamic magnetic field in the sample. A magnetic vector potential A is defined as

$$B_d = \nabla \times A \quad (3)$$

where B_d is the dynamic magnetic field. If axial symmetry is assumed, the vector potential has only an azimuthal component, A_ϕ . For simplicity, A_ϕ is represented as A in the rest of the paper. The eddy current density is given by

$$J = -\sigma \frac{\partial A}{\partial t} \quad (4)$$

Therefore, the Lorentz force in the absence of an external static magnetic field is written as

$$\begin{aligned} F_d &= J \times B_d \\ &= -\sigma \frac{\partial A}{\partial t} \times (\nabla \times A) \end{aligned} \quad (5)$$

If the eddy current penetration depth is much smaller than the acoustic wavelength, the forces exerted by the eddy currents can be considered as surface forces [2]. In our case, we use a low frequency sinusoidal signal to excite the coil and skin depth is much smaller than the acoustic wavelength. Once the surface forces are known, the acoustic displacements due to the surface force can be computed using Green's function [15]. The expressions for vector potential, surface force and acoustic displacements can be found in the paper by Kawashima et al [2].

In this study, we follow the approach taken by Kawashima *et al* [2] to theoretically compute the acoustic displacements produced by Lorentz force due to dynamic magnetic field in the metallic sample. As an example, in copper, the acoustic displacement at an excitation frequency of 85 kHz and a current of 100 mA, using an electromagnetic coil with a diameter of 7 mm and 100 turns of copper wire was found to be approximately 1 nm. While detection of nm displacements is quite difficult with piezoelectric transducers and EMAT, an AFM can detect displacements in nanometer range. Hence, AFM has a potential to detect ultrasonic amplitudes generated by eddy currents in a metal without the presence of an external static magnetic field.

EXPERIMENTAL METHOD

Figure 1 shows a schematic of the experimental setup used for the detection and measurement of acoustic displacements. The sample is placed in a time-varying magnetic field generated by a coil of diameter a , excited at a frequency f . The eddy currents generated in the metal give rise to a dynamic magnetic field. The eddy current field interacts with the dynamic magnetic field producing Lorentz forces. The body forces due to the Lorentz forces in the sample generate longitudinal acoustic displacements. A

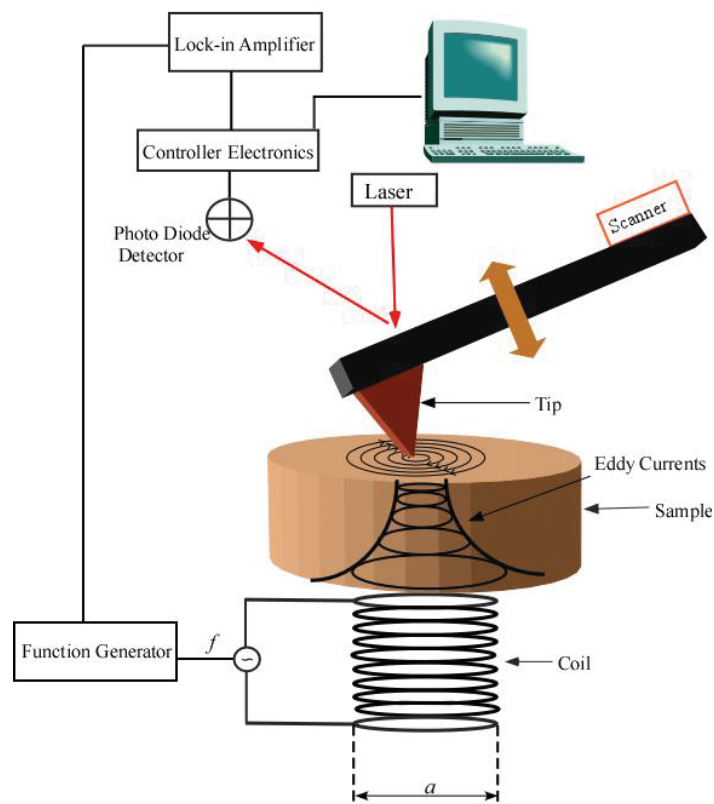


FIGURE 1. Experimental setup for the measurement and imaging of acoustic fields generated by eddy currents using an AFM.

flexible cantilever (spring constant, 0.12 N/m) with a nonmagnetic tip is brought into contact with the sample surface and scanned. The coil excitation frequency is chosen in such that the frequency matches the resonant frequency of the AFM cantilever for maximum sensitivity. The oscillation of the cantilever is detected by a four-quadrant photo diode detector of the AFM. The output of the photodiode detector is fed into one arm of the lock-in amplifier, while the output of the function generator exciting the coil at frequency f is fed to the second arm. The output of the lock-in amplifier provides measurements of amplitude of the acoustic displacements which are used to produce acoustic images.

RESULTS AND DISCUSSION

Detection of Acoustic Amplitude in Single Crystal Copper

The acoustic amplitudes due to the eddy currents were measured using an AFM in a single crystal copper as a function of excitation current. The sample was polished flat and parallel to a metallographic finish. The final polish was performed with 0.25 μm colloidal silica solution in a vibromet for at least an hour. A Digital Instruments Dimension 3000 AFM was used for the experiments. During the experiment, the sample was placed on a small coil and was excited at 85 kHz sinusoidal signal. The non-magnetic AFM cantilever-tip was brought into contact with the sample and the displacement of the cantilever was measured as the current was varied from zero to about 120 mA.

Figure 2 shows the acoustic displacement measured using the AFM cantilever as a function of input current to the coil in single crystal copper. The plot also shows theoretically computed acoustic displacements in the copper. While the amplitudes of the

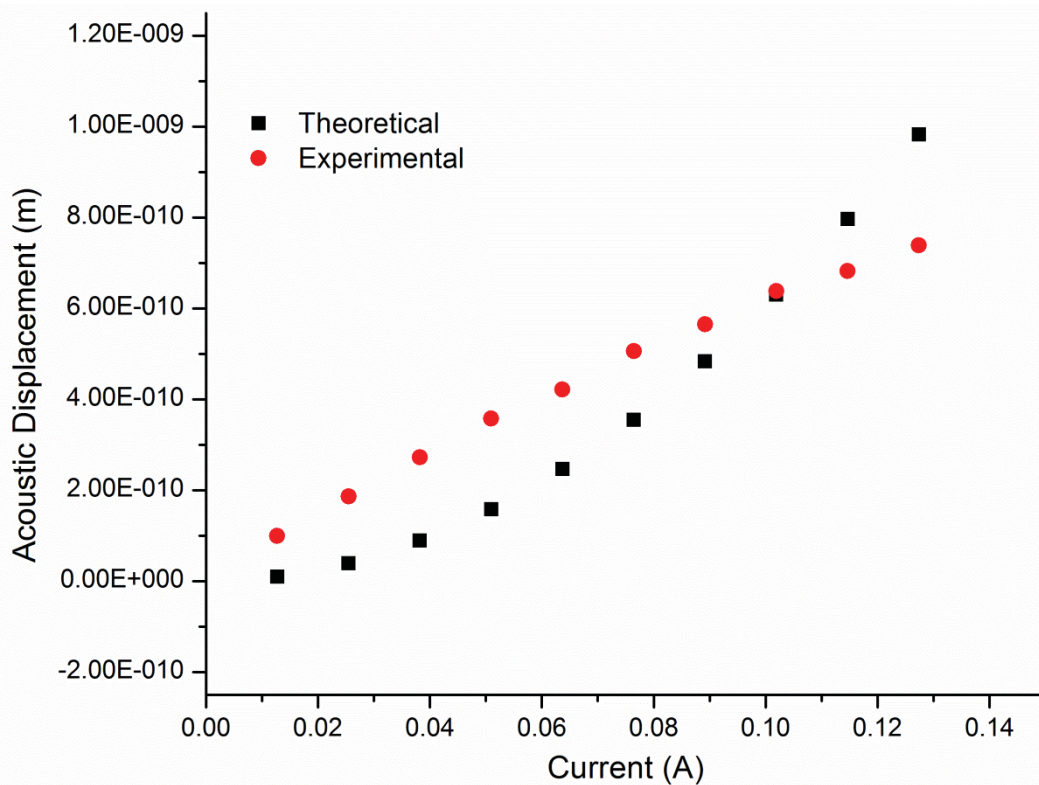


FIGURE 2. Comparison of theoretical and experimental acoustic displacements in a single crystal copper as a function of input current to the coil.

acoustic displacements were in the same order of magnitude, there is a significant difference in the behavior of the curves for the theoretical and experimental displacements. The experimental acoustic displacements show a linear behavior as a function of the input current. The maximum amplitude that was measured is about 700 pm. On the other hand, the theoretical displacement shows a quadratic behavior as a function of input current. The maximum amplitude is about 900 pm. The difference in the theoretical and experimental data may be attributed to the dimensions of the sample, detection of the field by AFM and assumptions made in theoretical computation of the displacement. Theoretical evaluation is based on infinite thickness of the sample, while the sample used in the experiments has a thickness very small compared to the acoustic wavelength. This may cause the sample to produce other types of vibrations. A theoretical computation of acoustic fields is usually determined in the far field of the transducer, while experimental measurement is performed in the near field using AFM.

Imaging Acoustic Fields in Titanium Alloy

As an application of the method for acoustic imaging, a sample of Ti-6Al-4V was used to image the microstructure. Ti-6Al-4V is a dual phase alloy with α phase hexagonal close pack crystallographic (HCP) structure and a lamellar structure consisting of alternate α and body center cubic (BCC) β phases. The average grain size of the sample used in the experiment was 20 μm . The volume fraction of the primary α phase is 60%, the volume fraction of α phase in the lamellar structure is 35%, and the remaining 5% is the β phase. The β is forms as a thin layer $<1 \mu\text{m}$ between the platelets of α in the lamellar structure. Figure 3 shows surface topography and acoustic displacement image of the same area of the sample with a scan area of 100 $\mu\text{m} \times 100 \mu\text{m}$. The image was obtained with a

sinusoidal signal with a frequency of 86 kHz and 110mA current is used to excite the eddy current coil under the sample, and the AFM tip was in contact with the top surface detecting the acoustic displacements. The surface topography image (Fig 3a) and the acoustic displacement image (Fig 3b) were acquired at the same time. The average surface roughness across the image is far less than 1 μm . The surface topography contrast shows that the primary alpha, the alpha platelets and the β phase between the alpha plates. The primary alpha grains appear to have uniform surface topography and hence there little variation in the contrast. On the other hand the lamellar grains have significant topography variation. The difference in topography may be due to different hardness and amount of material removed during polishing. The primary α phase grains appear with slightly different acoustic displacements, whereas the surface topography is fairly uniform contrast. This may be due to the differences in elastic modulus and electrical conductivity in different grains and crystallographic orientation. A closer inspection of both the images reveals differences in the contrast in the acoustic image. The contrast in the surface topography of Fig 3a of large primary α grains is quite uniform. In the acoustic displacement image shown in Fig 3b, the contrast is different for different grains. The grains that appear to be single in surface topography appear to consist of multiple grains. From the theoretical arguments, the contrast in the acoustic displacement image is due to the combination of elastic modulus and the electrical conductivity of the material under the AFM tip. The α phase in Ti-6Al-4V has a HCP crystal structure. Hence its elastic modulus and electrical conductivity are anisotropic. The contrast among the α grains in the image is due to difference in crystallographic orientation, elastic modulus and electrical conductivity anisotropy.

SUMMARY

This paper has presented detection and imaging of acoustic fields, generated by low-frequency electromagnetic fields, in metallic samples without the presence of an external static magnetic field. In the absence of an external static magnetic field, the acoustic displacements due to dynamic magnetic fields in the metallic sample were theoretically computed to be in the range of few hundred picometers. AFM was used to detect and image acoustic fields generated by an electromagnetic coil placed below the sample. Eddy current generated acoustic field displacements were experimentally measured in a single crystal copper as a function of input current to the coil and compared

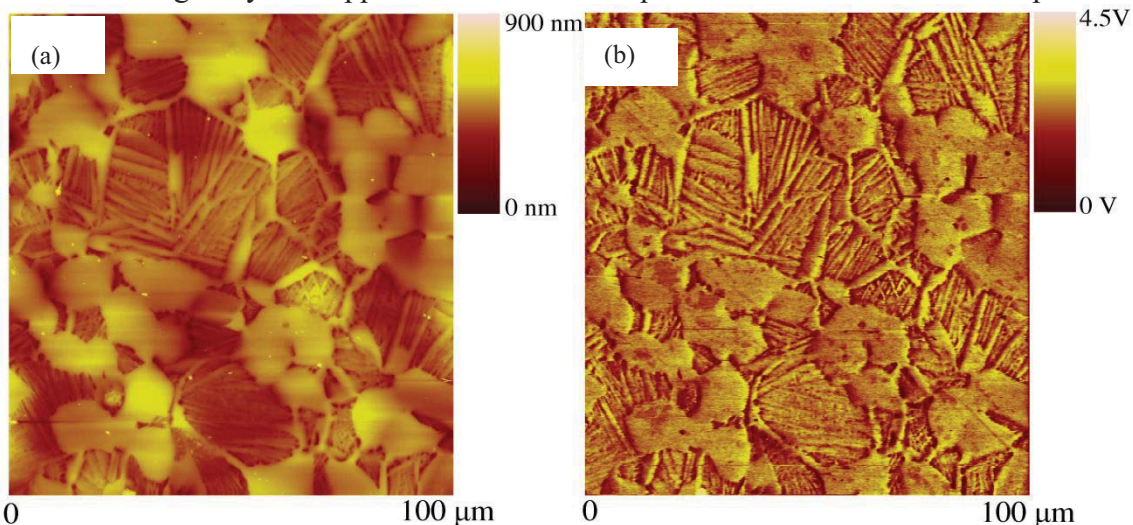


FIGURE 3. (a) Surface topography showing the primary α grains and lamellar β phase in Ti-6Al-4V (b) Corresponding acoustic field image of the same area.

with theoretical computations. AFM was also used to obtain the surface topography and acoustic field images of a titanium alloy, Ti-6Al-4V simultaneously. The surface topography image shows a uniform contrast in the primary α grains. However, the acoustic field image of the same grains show contrast from grain to grain and also within a grain. The contrast seen in the acoustic images is explained based on the elastic and electrical anisotropy of the α phase of the titanium alloy.

ACKNOWLEDGEMENTS

V. Nalladega acknowledges the financial support of the Dayton Area Graduate Studies Institute (DAGSI). The authors acknowledge the financial support from AFRL, Wright-Patterson Air Force Base, for this study under contract # FA8650-09-D5224, F33615-03-3-9001 and F33615-03-C-5219.

REFERENCES

1. E. R. Dobbs, "Electromagnetic Generation of Ultrasonic Waves," in *Physical Acoustics* Vol. 10, edited by W. P. Mason and R. N. Thurston, Academic, New York, 1973.
2. K. Kawashima, *J. Acoust. Soc. Am.* **60**, pp. 1089-1099 (1976).
3. B. W. Maxfield and C. M. Fortunko, *Mat. Eval.* **41**, pp. 1399-1408 (1983).
4. B. W. Maxfield, A. Kuramoto, and J. K. Hulbert, *Mat. Eval.* **45** pp. 1166-1183 (1987).
5. X. Jian, S. Dixon, K. T. V. Grattan, and R. S. Edwards, *Sensors and Actuators A*, **128** pp. 296-304 (2006).
6. R. B. Thompson, "Physical Principles of Measurements with EMAT Transducers," in *Physical Acoustics* Vol. 19, edited by R. N. Thurston and A. D. Pierce, Academic, New York, 1990, pp. 157-200.
7. M. Hirao and H. Ogi, *EMATs for Science and Industry: Noncontacting Ultrasonic Measurements*, Kluwer Academic, Dordrecht, 2003.
8. R. Ribichini, "Modelling of Electromagnetic Acoustic Transducers," PhD Thesis, Imperial College London, (2011).
9. X. Jian, S. Dixon, R. S. Edwards, and J. Reed, *J. Acoust. Soc. Am.* **119** pp. 2693-2701 (2006).
10. K. Kawashima, S. Murota, Y. Nakamori, H. Soga, and H. Suzuki, "Electromagnetic Generation of Ultrasonic Waves in Absence of External Magnetic Field and its Applications to Steel Production Lines," in *Proc. 9th World Conf. on Nondestructive Testing*, 4H-3, pp. 1-8.
11. G. Binnig, C. F. Quate, and Ch. Gerber, *Phys. Rev. Lett.* **56** pp. 930-933 (1986).
12. S. Hirsekorn, U. Rabe, A. Boub, and W. Arnold, *Surf. Interface Anal.* **27** pp. 474-481 (1999).
13. V. Nalladega, S. Sathish, K. V. Jata, and M. P. Blodgett, *Rev. Sci. Instrum.* **79** 073705 (2008).
14. V. Nalladega, S. Sathish, and A. S. Brar, *Microelectronics Reliability*, **48** pp. 1683-1688 (2008).
15. L. R. Johnson, *Geophys. J. Roy. Astron. Soc.* **37** pp. 99-131 (1974).